ULTRA SONO GRAPHY

Advanced fibrosis leads to overestimation of steatosis with quantitative ultrasound in individuals without hepatic steatosis

Takashi Kumada[1], Hidenori Toyoda[2], Sadanobu Ogawa[3], Tatsuya Gotoh[3], Yasuaki Suzuki[4], Kento Imajo[5,6], Katsutoshi Sugimoto[7], Tatsuya Kakegawa[7], Hidekatsu Kuroda[8], Yutaka Yasui[9], Nobuharu Tamaki[9], Masayuki Kurosaki[9], Namiki Izumi[9], Tomoyuki Akita[10], Junko Tanaka[10], Atsushi Nakajima[5]

※ Author affiliations appear at the end of this article.

ORIGINAL ARTICLE

https://doi.org/10.14366/usg.23194
eISSN: 2288-5943
Ultrasonography 2024;43:121-131

Purpose: The effect of hepatic fibrosis stage on quantitative ultrasound based on the attenuation coefficient (AC) for liver lipid quantification is controversial. The objective of this study was to determine how the degree of fibrosis assessed by magnetic resonance (MR) elastography affects AC based on the ultrasound-guided attenuation parameter according to the grade of hepatic steatosis, using magnetic resonance imaging (MRI)–derived proton density fat fraction (MRI-derived PDFF) as the reference standard.

Methods: Between February 2020 and April 2021, 982 patients with chronic liver disease who underwent AC and MRI-derived PDFF measurement as well as MR elastography were enrolled. Multiple regression was used to investigate whether AC was affected by the degree of liver stiffness.

Results: AC increased as liver stiffness progressed in 344 patients without hepatic steatosis (P=0.009). In multivariable analysis, AC was positively correlated with skin-capsule distance (P<0.001), MR elastography value (P=0.037), and MRI-derived PDFF (P<0.001) in patients without hepatic steatosis. In 52 of 982 patients (5%), the correlation between AC and MRI-derived PDFF fell outside the 95% confidence interval for the regression line slope. Patients with MRI-derived PDFF lower than their AC (n=36) had higher fibrosis-4 scores, albumin-bilirubin scores, and MR elastography values than patients with MRI-derived PDFF greater than their AC (n=16; P=0.018, P=0.001, and P=0.011, respectively).

Conclusion: AC is affected by liver fibrosis (MR elastography value ≥6.7 kPa) only in patients without hepatic steatosis (MRI-derived PDFF <5.2%). These values should be interpreted with caution in patients with advanced liver fibrosis.

Keywords: Hepatic steatosis; Attenuation coefficient; MR elastography; MRI-derived proton density fat fraction; Liver stiffness

Key points: Attenuation coefficient (AC) measured with the ultrasound-guided attenuation parameter is affected by advanced liver fibrosis in patients without steatosis. AC was positively associated with skin-capsule distance (P<0.001), magnetic resonance elastography value (P=0.021), and magnetic resonance imaging–derived proton density fat fraction (P<0.001) in patients without liver steatosis. ACs should be interpreted with caution in patients with advanced liver fibrosis who do not have steatosis.

Received: October 19, 2023
Revised: December 11, 2023
Accepted: December 11, 2023

Correspondence to:
Takashi Kumada, MD, Department of Nursing, Faculty of Nursing, Gifu Kyoritsu University, 5-50, Kitagata-cho, Ogaki-shi, Gifu-ken, 503-8550, Japan

Tel. +81-584-77-3512
Fax. +81-584-77-3510
E-mail: takashi.kumada@gmail.com

How to cite this article:
Kumada T, Toyoda H, Ogawa S, Gotoh T, Suzuki Y, Imajo K, et al. Advanced fibrosis leads to overestimation of steatosis with quantitative ultrasound in individuals without hepatic steatosis. Ultrasonography. 2024 Mar;43(2):121-131.

Introduction

Non-alcoholic fatty liver disease (NAFLD) is the most common cause of chronic liver disease; it is present in approximately 30% of the general population [1]. NAFLD, and hepatitis B virus (HBV) and hepatitis C virus (HCV) coinfection are associated with an increased risk of liver cirrhosis and hepatocellular carcinoma [2]. The diagnosis of hepatic steatosis has thus become clinically important.

The current standard for quantification of hepatic steatosis is histologic evaluation by a pathologist. Quantification of hepatic steatosis in histological sections is strongly observer-dependent, not reproducible, and not correlated with computerized estimation [3]. Due to the known spatial heterogeneity of diffuse liver disease, limited sampling of the liver might lead to errors in diagnosis, staging, and prognosis [4,5]. To reduce the need for biopsies, various imaging biomarkers have emerged as non-invasive tools for the diagnosis and monitoring of patients with hepatic steatosis. Magnetic resonance imaging (MRI)–derived proton density fat fraction (PDFF), which reflects hepatic triglyceride content, has been shown to be accurate and reproducible for quantifying hepatic steatosis. Based on the observation that changes in hepatic steatosis might be associated with changes in other histological endpoints, MRI-derived PDFF is currently being used as a primary or secondary endpoint in several early-stage clinical trials [6,7]. MRI-derived PDFF is even more accurate than liver biopsy for liver fat quantification [8]. However, using MRI-derived PDFF to monitor large numbers of individuals at risk for hepatic steatosis would be costly and practically challenging.

Recently, various quantitative ultrasound (US) techniques that characterize tissue microstructure using the attenuation coefficient (AC, measured in units of dB/cm/MHz) have been developed and validated for the diagnosis of hepatic steatosis [9–15]. However, the impact of hepatic fibrosis stage on quantitative US results based on the AC is uncertain [10–13]. We hypothesized that AC based on ultrasound-guided attenuation parameter (UGAP) might be influenced by the grade of liver fibrosis, as our previous study showed a wide range of MRI-derived PDFFs in patients who were judged not to have hepatic steatosis based on AC [9]. Thus, we aimed to clarify the effect of fibrosis stage on AC as a biomarker for liver fat quantification. The purpose of our study was to determine how the degree of hepatic fibrosis assessed by magnetic resonance (MR) elastography affects AC according to the grade of hepatic steatosis using MRI-derived PDFF as the reference standard.

Materials and Methods

Compliance with Ethical Standards

This study was approved by the institutional review board of Ogaki Municipal Hospital (approval number 20190822-6) and carried out in compliance with the Declaration of Helsinki. This prospective study was approved by six institutional review boards (Ogaki Municipal Hospital, Nayoro City General Hospital, Yokohama City University Hospital, Tokyo Medical University Hospital, Iwate Medical University Hospital, and Japanese Red Cross Musashino Hospital). It was registered in the University Hospital Medical Information Network (UMIN) Clinical Trials Registry (UMIN000041196), and informed consent was obtained from all participants.

Study Population

Consecutive patients who underwent quantitative US assessment based on the AC between February 2020 and April 2021 at six liver hospitals were prospectively enrolled. Inclusion criteria consisted of age ≥18 years, chronic liver disease (known non-alcoholic fatty liver disease, alcoholic liver disease, HBV or HCV infection, autoimmune hepatitis, primary biliary cholangitis, or other), and willingness and ability to participate. Exclusion criteria consisted of contraindication for MRI due to metal in the body or claustrophobia, or no MR elastography examination.

Alanine aminotransferase, aspartate aminotransferase, platelet count, albumin, and total bilirubin were measured at the time of AC assessment. The albumin-bilirubin (ALBI) score and fibrosis-4 (FIB-4) score were also evaluated [16,17].

Ultrasound-Guided Attenuation Parameter

AC was measured using a LOGIQ E10 ultrasound system (GE Healthcare [9]). Each center used their own LOGIQ E10 ultrasound system. The six equipment units were adjusted in a phantom experiment to produce identical ACs before shipment [18,19]. Each scan was performed within 3 months of MRI-derived PDFF and MR elastography assessment after fasting for more than 4 hours. Patients were placed in the supine position with the right arm in maximum abduction. Sonographers, who had more than 5 years of experience with US, were unaware of the MRI-derived PDFF findings of each patient. Using an intercostal approach, a large color-coded attenuation map was automatically generated and adjusted by the system in a homogeneous region of liver segment VII or VIII that was free of large vessels. The best image was selected using the quality map option to determine AC (dB/cm/MHz). At least five measurements were performed; AC was estimated from B-mode images and automatically stored in the system [20,21]. Reliable AC was defined as the median of five measurements obtained with

an interquartile-to-median ratio <0.30 for liver fat content [22]. Steatosis was categorized as grade 0 (S0) for AC <0.65 dB/cm/MHz, grade 1 (S1) for 0.65 dB/cm/MHz≤AC<0.71 dB/cm/MHz, grade 2 (S2) for 0.71 dB/cm/MHz≤AC<0.77 dB/cm/MHz, and grade 3 (S3) for AC ≥0.77 dB/cm/MHz [9].

MRI-Derived PDFF and MR Elastography

MRI was performed using a 3-T system (Discovery MR750w 3.0 T, GE Healthcare). MRI-derived PDFF was measured using the multi-echo Dixon method (IDEAL-IQ sequence). MRI-derived PDFF measurement and MR elastography were performed as described previously [9,23,24]. Steatosis grade was categorized as grade 0 (S0) for MRI-derived PDFF <5.2%, grade 1 (S1) for 5.2%≤MRI-derived PDFF<11.3%, grade 2 (S2) for 11.3%≤MRI-derived PDFF<17.1%, and grade 3 (S3) for MRI-derived PDFF ≥17.1% [23]. MR elastography values were recorded in kilopascal (kPa). Fibrosis stage was defined as F0 for MR elastography value <2.5 kPa, F1 for 2.5 kPa≤MR elastography value<3.4 kPa, F2 for 3.4 kPa≤MR elastography value<4.8 kPa, F3 for 4.8 kPa≤MR elastography value<6.7 kPa, and F4 for MR elastography value >6.7 kPa [23].

Image Analysis

After image acquisition, MRI-derived PDFF and MR elastography values for each patient were independently evaluated by technologists with more than 5 years of experience in MRI in each department's imaging postprocessing laboratory. Each technologist measured MRI-derived PDFF by placing a single region of interest (ROI) on imager-generated parametric fat maps. They were blinded to the results of the other reviewers and to the patient's AC and other MRI-derived PDFF measurements. A hepatologist at each institution with more than 10 years of experience in MRI and US interpretation checked the anatomically co-located AC and MRI-derived PDFF ROIs and decided which values calculated by the independent readers should be used. If more than one value was determined to be appropriate, the average value was used.

Statistical Analysis

Continuous variables are expressed as medians (interquartile range, IQR). The Mann-Whitney U test, Kruskal-Wallis test, or Jonckheere-Terpstra test was used to assess continuous variables. Post hoc analysis was performed with the Steel-Dwass test if the Kruskal-Wallis test showed a significant difference. The Jonckheere-Terpstra test is a test for ordered alternative hypotheses within an independent sample (between-patients) design. The chi-square test or Fisher's exact test was used to analyze categorical variables. In this study, AC was the dependent variable. Independent variables consisted of age, sex, body mass index (BMI), skin-capsule distance (SCD), MR elastography value, MRI-derived PDFF, and MR elastography value×MRI-derived PDFF. Factors that were not significant in the univariate analysis (i.e., P≥0.1) were not included in the multiple regression analysis. Shapiro-Wilk tests were used to determine whether these parameters were normally distributed; if not, they were log-transformed to achieve a normal distribution. MR elastography and MRI-derived PDFF values were centralized (i.e., the mean value was subtracted from each value) and divided by the standard deviation to avoid multicollinearity. The variance inflation factor (VIF) was used to assess multicollinearity in multiple regression models. VIF >4.00 was considered to indicate multicollinearity [25]. Statistical significance was defined as P<0.05. All statistical analyses were performed with EZR (version 1.61, Saitama Medical Center, Jichi Medical University, Saitama, Japan) [26].

Results

Patient Characteristics

We enrolled 982 patients (Fig. 1). The median age was 64 years (IQR, 52 to 72). There were 457 females (46.5%) and 525 males (53.5%). All patients were Japanese and Asian. Table 1 shows the baseline characteristics of the study participants. Causes of chronic liver disease included NAFLD (n=497), alcoholic liver disease (n=85), HBV infection (n=129), HCV infection (n=122), autoimmune hepatitis (n=38), primary biliary cholangitis (n=44), and other

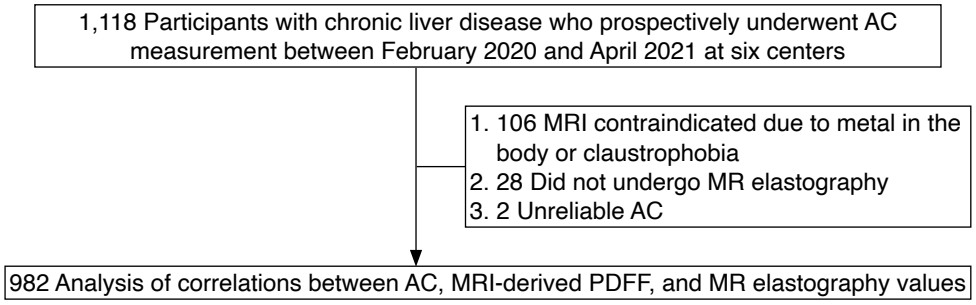

Fig. 1. Flowchart of the patient selection process. AC, attenuation coefficient based on the ultrasound-guided attenuation parameter; MRI, magnetic resonance imaging; MR, magnetic resonance; PDFF, proton density fat fraction.

Table 1. Baseline characteristics of the study participants (n=982)

Characteristic	Value
Cause of liver disease	
NAFLD	497 (50.6)
ALD	85 (8.7)
HBV	129 (13.1)
HCV	122 (12.4)
AIH	38 (3.9)
PBC	44 (4.5)
Other	67 (6.8)
Age (year)	64 (52–72)
Sex	
Women	457 (46.5)
Men	525 (53.5)
Body mass index (kg/m^2)	25.6 (23.1–28.8)
Skin capsular distance (mm)	19 (15–22)
Alcohol abuse	
Present	144 (14.7)
Absent	838 (85.3)
Smoking	
Present	235 (23.9)
Absent	747 (76.1)
Platelet count (×10^4/μL)	20.4 (15.6–24.9)
AST (U/L)	31 (23–48)
ALT (U/L)	35 (20–61)
FIB-4 score	1.04 (0.72–1.55)
γ-GT (U/L)	43 (25–80)
Total bilirubin (mg/dL)	0.8 (0.6–1.0)
Albumin (g/dL)	4.4 (4.1–4.6)
ALBI score	−3.00 (−3.19 to −2.75)
USAP value (dB/cm/MHz)	0.70 (0.60–0.78)
MRI-derived PDFF (%)	7.6 (3.7–15.2)
Without hepatic steatosis (MRI-derived PDFF <5.2%)	344 (35.0)
With hepatic steatosis (MRI-derived PDFF ≤5.2%)	638 (65.0)
MR elastography value (kPa)	2.7 (2.1–3.8)
Without hepatic fibrosis (MR elastography ≥2.5 kPa)	484 (49.3)
With hepatic fibrosis (MR elastography ≥2.5 kPa)	498 (50.7)

Values are presented as number (%) or median (interquartile range).
Steatosis grade: S0, MRI-derived PDFF <5.2%; S1, 5.2≤MRI-derived PDFF<11.3%; S2, 11.3≤MRI-derived PDFF<17.1%; and S3, MRI-derived PDFF ≥17.1% [12].
Fibrosis grade: F0, MR elastography value <2.5kPa; F1, 2.5≤MR elastography value<3.4 kPa; F2, 3.4≤MR elastography value<4.8 kPa; F3, 4.8≤MR elastography value<6.7 kPa; and F4, MR elastography value ≥6.7 kPa [12].
NAFLD, non-alcoholic fatty liver disease; ALD, alcoholic liver disease; HBV, hepatitis B virus; HCV, hepatitis C virus; AIH, autoimmune hepatitis; PBC, primary biliary cholangitis; AST, aspartate aminotransferase; ALT, alanine aminotransferase; FIB-4, fibrosis-4; γ-GT, gamma-glutamyl transpeptidase; ALBI, albumin-bilirubin; USAP, ultrasound attenuation parameter; MRI, magnetic resonance imaging; PDFF, proton density fat fraction.

(n=67). The median FIB-4 score was 1.04 (IQR, 0.72 to 1.55). The median ALBI score was −3.00 (IQR, −3.19 to −2.75). The median AC value was 0.70 dB/cm/MHz (IQR, 0.60 to 0.78). The median MRI-derived PDFF value was 7.6% (IQR, 3.7 to 15.2). There were 344 patients (35.0%) without hepatic steatosis and 638 patients (65.0%) with hepatic steatosis. The median MR elastography value was 2.7 kPa (IQR, 2.1 to 3.8). There were 484 patients (49.3%) without hepatic fibrosis and 498 patients (50.7%) with hepatic fibrosis.

Correlation between AC and MR Elastography Values Based on MRI-Derived PDFF

Fig. 2A shows ACs in patients classified as S0 (MRI-derived PDFF <5.2%, n=344) according to hepatic fibrosis grade based on MR elastography. AC was positively correlated with fibrosis grade (F0: 0.58 [IQR, 0.53 to 0.62], F1: 0.56 [IQR, 0.52 to 0.62], F2: 0.59 [IQR, 0.54 to 0.63], F3: 0.58 [IQR, 0.55 to 0.65], F4: 0.61 [IQR, 0.57 to 0.66]; P=0.009, Jonckheere-Terpstra test). By contrast, there were no significant correlations between AC and MR elastography values in patients with S1–S3 steatosis (MRI-derived PDFF >5.2%; P=0.09, Jonckheere-Terpstra test) (Fig. 2B). Among patients classified as S0 (MRI-derived PDFF <5.2%, n=344), 18 of 68 patients (26.5%) with advanced fibrosis (MR elastography value ≥6.7 kilopascal [kPa]) were misdiagnosed with S1–S3 steatosis (AC ≥0.65 dB/cm/MHz), while 43 of 276 patients (15.6%) without advanced fibrosis (MR elastography value <6.7 kPa) were misdiagnosed with S1–S3 steatosis (AC ≥0.65 dB/cm/MHz, P=0.049).

Univariable and Multivariable Analyses of Factors Associated with AC

Results of univariable and multiple regression analyses that included age, sex, BMI, MR elastography value, MRI-derived PDFF, and MR elastography value×MRI-derived PDFF stratified by AC are shown in Table 2.

In multiple regression analysis, AC (dB/cm/MHz) was positively correlated with SCD (estimate, 0.004; P<0.001) and MRI-derived PDFF (estimate, 0.082; P<0.001) and inversely correlated with age (estimate, −0.001; P<0.001) (Table 2). AC was associated with the interaction between MR elastography value and MRI-derived PDFF in all patients (estimate, −0.006; P=0.002) (Table 2). VIF values were 1.255 for age, 1.029 for sex, 2.057 for BMI, 1.760 for SCD, 1.146 for MR elastography value, and 1.523 for MRI-derived PDFF. AC was positively correlated with SCD (estimate, 0.005; P<0.001), MR elastography value (estimate, 0.009; P=0.021), and MRI-derived PDFF (estimate, 0.016; P<0.001) in patients without hepatic steatosis (Table 2). AC was positively correlated with SCD (estimate, 0.002; P<0.001) and MRI-derived PDFF (estimate, 0.057; P<0.001)

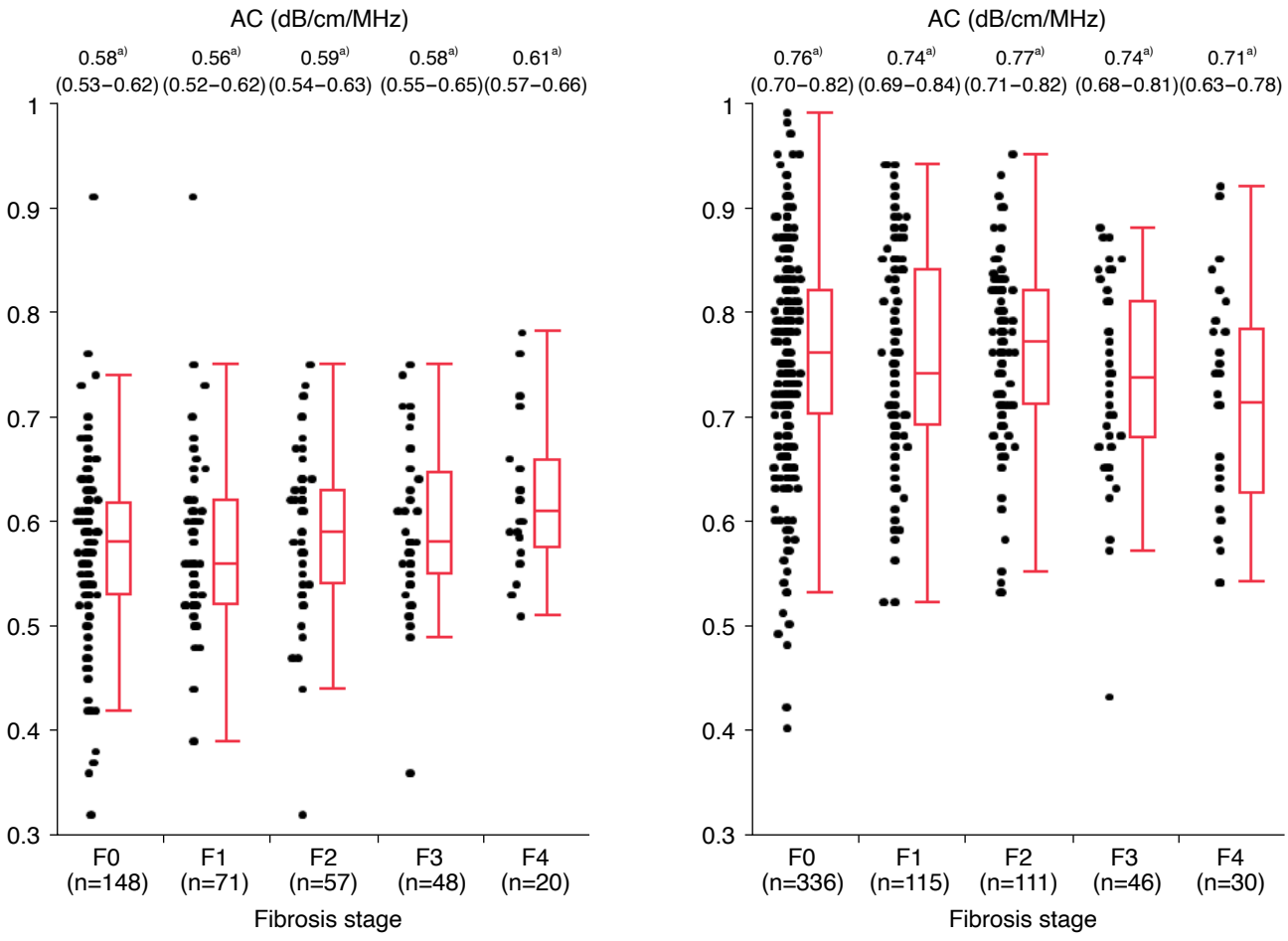

Fig. 2. AC and fibrosis stage according to MR elastography values stratified by the grade of hepatic steatosis based on MRI-derived PDFF.

A. AC by fibrosis grade (F0–F4) in patients without hepatic steatosis (S0, n=344, MRI-derived PDFF <5.2%) is shown. AC was positively correlated with fibrosis stage (P=0.009, Jonckheere-Terpstra test). B. AC by fibrosis grade (F0–F4) in patients with hepatic steatosis (S1–S3, n=638, MRI-derived PDFF ≥5.2%) is shown. AC was not correlated with fibrosis stage (P=0.088, Jonckheere-Terpstra test). [a]Median (IQR) AC by fibrosis stage. Fibrosis grade: F0, MR elastography value <2.5 kPa; F1, 2.5 kPa≤MR elastography value<3.4 kPa; F2, 3.4 kPa≤MR elastography value<4.8 kPa; F3, 4.8 kPa≤MR elastography value<6.7 kPa; and F4, MR elastography value ≥6.7 kPa [23]. Steatosis grade: S0, MRI-derived PDFF <5.2%; S1, 5.2%≤MRI-derived PDFF<11.3%; S2, 11.3%≤MRI-derived PDFF<17.1%; and S3, MRI-derived PDFF ≥17.1% [23]. AC, attenuation coefficient based on the ultrasound-guided attenuation parameter; IQR, interquartile range; MR, magnetic resonance; MRI, magnetic resonance imaging; PDFF, proton density fat fraction.

and inversely correlated with age (estimate, −0.001; P=0.001) in patients with hepatic steatosis (Table 2).

Patients with Discordant AC and MRI-Derived PDFF Findings

Intrarater and interrater reliability for AC were 0.99 and 0.95, respectively (Supplementary Table 1). Fig. 3 shows the correlation between AC and log MRI-derived PDFF values. The red dotted line indicates the upper limit for the 95% confidence interval (CI). The blue dotted line indicates the lower limit for the 95% CI. Of the 982 patients, 52 (5.3%) were outside of the 95% CI for the correlation coefficient. Group A (n=16) was defined as the group above the red dotted line (log MRI-derived PDFF value > AC). Group C (n=36) was defined as the group below the blue dotted line (log MRI-derived PDFF value <AC). The remaining patients were classified into group B (n=930). There was no evidence of statistical differences between groups A and B in any of the factors examined, except for AC (dB/cm/MHz, 0.55 [IQR, 0.48 to 0.65] vs. 0.70 [IQR, 0.60 to 0.79], P=0.003) and MRI-derived PDFF (17.6 [IQR, 8.7 to 21.2] vs. 2.7 [IQR, 2.1 to 3.8], P<0.001) (Table 3, Supplementary Table 2). The FIB-4 score was significantly higher in group C than in group B (1.03

Table 2. Univariable and multivariable analysis of factors associated with the USAP value as a continuous variable in linear regression analysis

Parameter	Univariable analysis		Multiple regression analysis		
	Pearson r	P-value	Estimate[a]	Standard error	P-value
All patients (n=982)					
Age (year)	−0.349	<0.001	−0.001	0.000	<0.001
Sex[a]	0.074	0.021	0.004	0.005	0.008
BMI (kg/m^2)	0.513	<0.001	0.002	0.001	0.020
SCD (mm)	0.461	<0.001	0.004	0.001	<0.001
MR elastography	−0.054	0.091	0.008	0.003	0.004
MRI-derived PDFF	0.731	<0.001	0.078	0.003	<0.001
MR elastography×MRI-derived PDFF	−0.186	<0.001	0.009	0.004	0.013
Patients without hepatic steatosis (grade S0, n=344)					
Age (year)	−0.039	0.467	−0.000	0.000	0.480
Sex[a]	−0.015	0.788	−0.013	0.008	0.100
BMI (kg/m^2)	0.240	<0.001	−0.000	0.001	0.751
SCD (mm)	0.361	<0.001	0.006	0.001	<0.001
MR elastography	0.173	0.001	0.032	0.017	0.037
MRI-derived PDFF	0.084	0.122	0.061	0.021	<0.001
MR elastography×MRI-derived PDFF	−0.158	0.003	0.023	0.019	0.229
Patients with hepatic steatosis (grades S1−S3, n=638)					
Age (year)	−0.341	<0.001	−0.001	0.000	0.002
Sex[a]	0.057	0.154	0.006	0.006	0.317
BMI (kg/m^2)	0.331	<0.001	0.002	0.001	0.094
SCD (mm)	0.285	<0.001	0.002	0.001	0.004
MR elastography	−0.088	0.034	0.002	0.003	0.482
MRI-derived PDFF	0.604	<0.001	0.061	0.001	<0.001
MR elastography×MRI-derived PDFF	0.001	0.227	0.014	0.005	0.007

Estimated value of coefficients.

Steatosis grade: S0, MRI-PDFF <5.2%; S1, 5.2≤MRI-PDFF<11.3%; S2, 11.3≤MRI-PDFF<17.1%; and S3, MRI-PDFF ≥17.1% [12].

USAP, ultrasound attenuation parameter; BMI, body mass index; SCD, skin-capsule distance; MR, magnetic resonance; MRI, magnetic resonance imaging; PDFF, proton density fat fraction.

[a]Female=0, male=1.

[IQR, 0.71 to 1.54] vs. 1.33 [IQR, 0.85 to 1.93], P=0.017, Steel-Dwass test) (Table 3, Supplementary Table 2). ALBI scores and MR elastography values were significantly higher in group C than in groups A and B (−2.81 [IQR, −2.96 to −2.41] vs. −2.95 [IQR, −3.24 to −2.85], P=0.029 and vs. −3.00 [IQR, −3.20 to −2.76], P=0.001 for ALBI score and 3.3 [IQR, 2.4 to 5.2] vs. 2.3 [IQR, 2.0 to 2.9], P=0.019 and vs. 2.7 [IQR, 2.1 to 3.8], P=0.027 for MR elastography values, respectively; Steel-Dwass test) (Table 3, Supplementary Table 2). By contrast, BMI, AC, and MRI-derived PDFF were lower in group C than in group B (22.9 [IQR, 20.9 to 24.8] vs. 25.7 [IQR, 23.2 to 29.0], P<0.001; 0.62 [IQR, 0.59 to 0.67] vs. 0.70 [IQR, 0.60 to 0.79], P=0.006; and 1.4 [IQR, 1.1 to 1.7] vs. 8.6 [IQR, 4.9 to 15.8], P<0.001, respectively; Steel-Dwass test) (Table 3, Supplementary Table 2). Fig. 4 shows the results from a patient with non-viral cirrhosis in group C.

Discussion

The effect of hepatic fibrosis stage as assessed with quantitative US on the basis of AC is controversial. We demonstrated that quantitative US techniques based on AC are associated with an interaction between MR elastography value and MRI-derived PDFF in a large study sample (n=982). This multicenter prospective cross-sectional study showed that the grade of hepatic steatosis as assessed with AC is affected by advanced liver stiffness evaluated with MR elastography. After stratifying patients according to the

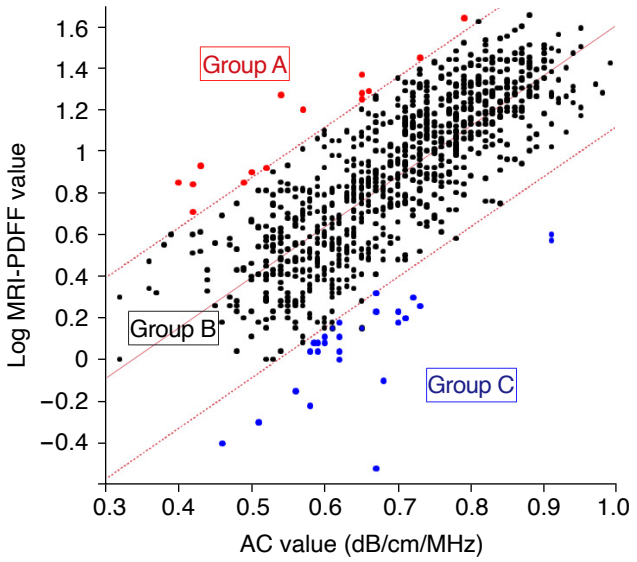

Fig. 3. Correlations between AC and log MRI-derived PDFF values. The correlation between AC and log MRI-derived PDFF values fell outside the 95% confidence interval for the slope of the regression line in 52 of 982 patients (5%). All patients were classified into the following three groups: group A (n=16), high MRI-derived PDFF and low AC; group B (n=930), concordant MRI-derived PDFF and AC; group C (n=36), low MRI-derived PDFF and high AC. AC, attenuation coefficient based on the ultrasound-guided attenuation parameter; MRI, magnetic resonance imaging; PDFF, proton density fat fraction.

stage of hepatic steatosis on the basis of MRI-derived PDFF, AC was positively correlated with fibrosis grade only in patients without hepatic steatosis (P=0.009), suggesting that hepatic fibrosis affects AC.

However, many studies, including studies about the controlled attenuation parameter (Echosens, Paris, France), attenuation imaging (Canon Medical Systems, Otawara, Japan), and UGAP, have reported that the presence of fibrosis does not affect AC [10–13]. Dioguardi Burgio et al. found no statistical evidence that ACs in patients with advanced fibrosis (F3–F4) are different from ACs in patients with F0–F2 fibrosis (0.72±0.13 vs. 0.70±0.13 dB/cm/MHz; P=0.38) [10]. An insufficient number of patients in these studies might have led to results that differed from those of this study. However, there are many reports showing that acoustic attenuation increases with both hepatic steatosis and fibrosis, which are the two most important findings observed in diffuse liver disease [27–30]. All these studies concluded that ACs depend mainly on fat and, to a lesser extent, fibrosis. It is difficult to explain the differential effect of liver fibrosis on various grades of hepatic steatosis. The effect of fat on AC is larger than the effect of fibrosis on AC [27–30]. We speculate that this is because the effect of fibrosis was observed in patients without hepatic steatosis, whereas the effect of fibrosis was counteracted in patients with hepatic steatosis. The degree of fibrosis likely does not affect the accuracy within the biologically relevant patients/range.

Table 3. Background factors of patients with a discrepancy between the UGAP value and MRI-PDFF

	Group A (n=16)	Group B (n=930)	Group C (n=36)	P-value
Age (year)	65 (48–69)	64 (52–72)	68 (55–73)	0.334
Female sex	9 (56.2)	428 (46.0)	20 (55.6)	0.390
Alcohol abuse (%)	5 (31.2)	133 (14.6)	6 (16.7)	0.170
Body mass index (kg/m^2)	27.9 (21.6–29.0)	25.7 (23.2–29.0)	22.9 (20.9–24.8)	<0.001
SCD (mm)	16 (13–19)	19 (16–22)	18 (13–20)	0.009
AST (U/L)	39 (27–67)	31 (23–48)	27 (20–38)	0.072
ALT (U/L)	38 (20–81)	35 (20–61)	23 (13–37)	0.004
Platelet count (×10^4/μL)	21.8 (14.5–25.2)	20.5 (15.7–25.1)	16.7 (12.5–21.4)	0.006
FIB-4 score	0.90 (0.73–1.49)	1.03 (0.71–1.54)	1.33 (0.85–1.93)	0.018
Total bilirubin (mg/dL)	0.8 (0.6–1.1)	0.8 (0.6–1.0)	0.8 (0.6–1.1)	0.489
Albumin (g/dL)	4.4 (4.2–4.6)	4.4 (4.1–4.6)	4.2 (3.8–4.4)	0.001
ALBI score	−2.95 (−3.24 to −2.85)	−3.00 (−3.20 to −2.76)	−2.81 (−2.96 to −2.41)	0.001
USAP value (dB/cm/MHz)	0.55 (0.48–0.65)	0.70 (0.60–0.79)	0.62 (0.59–0.67)	<0.001
MRI-derived PDFF (%)	17.6 (8.7–21.2)	8.6 (4.9–15.8)	1.4 (1.1–1.7)	<0.001
MR elastography value (kPa)	2.3 (2.0–2.9)	2.7 (2.1–3.8)	3.3 (2.4–5.2)	0.011

Values are presented as median (interquartile range) or number (%).
Group A (n=16), high MRI-derived PDFF values and low UGAP values; Group B (n=930), concordant MRI-derived PDFF and UGAP values; Group C (n=36), low MRI-derived PDFF and high UGAP values.
USAP, ultrasound attenuation parameter; MRI, magnetic resonance imaging; PDFF, proton density fat fraction; SCD, skin capsular distance; AST, aspartate aminotransferase; ALT, alanine aminotransferase; FIB-4, fibrosis-4; ALBI, albumin-bilirubin.

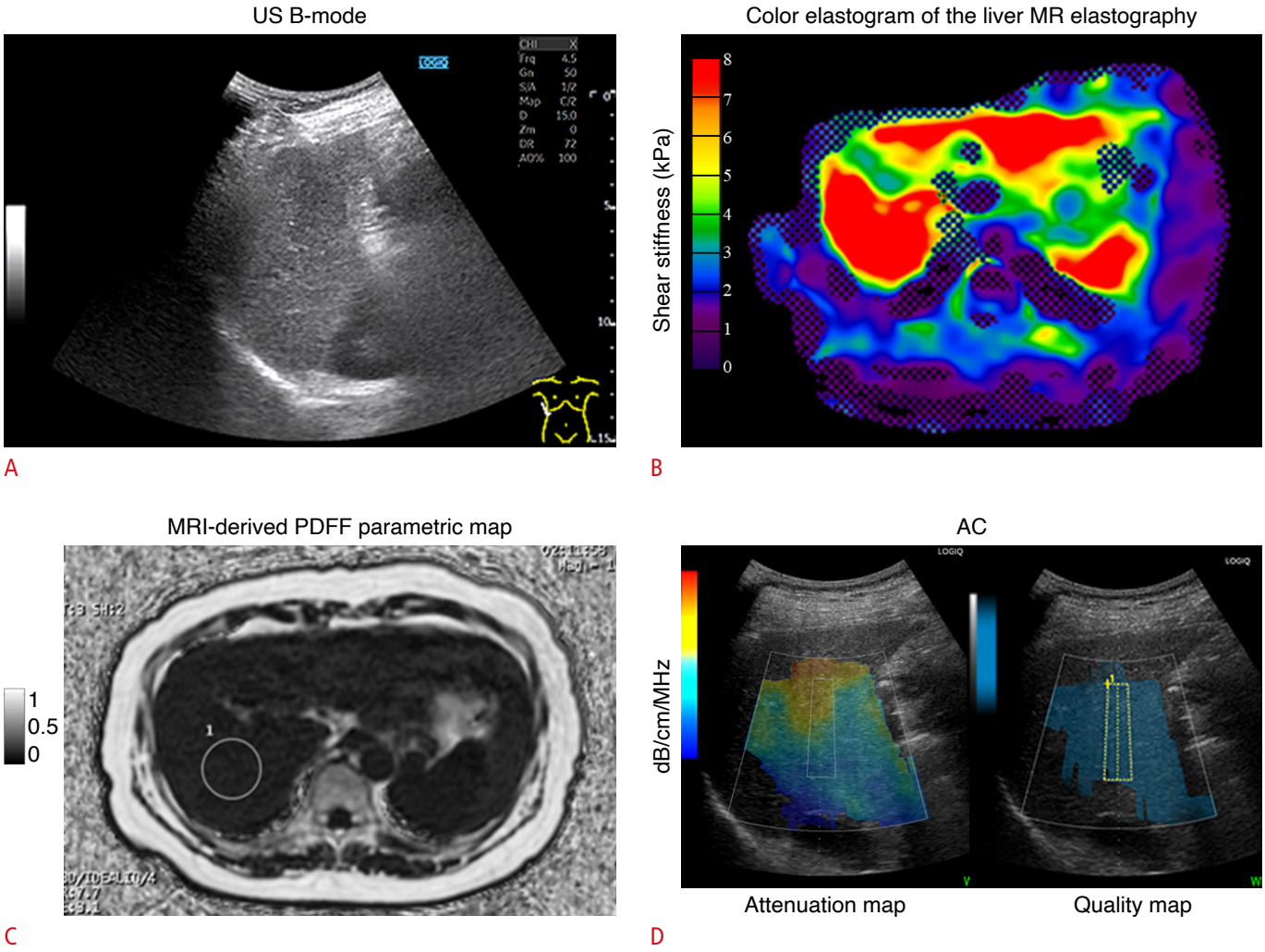

Fig. 4. A 56-year-old male outpatient with compensated cryptogenic cirrhosis who had no specific symptoms.
A. US B-mode shows a coarse speckle pattern in the liver parenchyma. The dynamic range was 72 dB. B. Color MR elastogram of the liver with a 95% confidence map is shown. Liver stiffness was 9.4 kPa, consistent with F4 fibrosis [23]. C. Parametric map of MRI-derived PDFF is shown. A single region of interest was placed in right posterior lobe of the liver. MRI-derived PDFF was 3.8%, consistent with S0 (no steatosis) [23]. D. ACs based on the ultrasound-guided attenuation parameter obtained during the same examination as the attenuation map on the left and a quality map on the right is shown. The attenuation map shows a suitable area for measuring the attenuation slope. If the measured signal contains structures such as blood vessels or the diaphragm, prediction error will be large and the attenuation map will show a dark color instead of blue. AC was 0.78 dB/cm/MHz, consistent with S3 (severe steatosis) [9]. This case demonstrates that AC overestimates hepatic steatosis in patients with F4 fibrosis [23]. AC, attenuation coefficient based on the ultrasound-guided attenuation parameter; MR, magnetic resonance; MRI, magnetic resonance imaging; PDFF, proton density fat fraction; US, ultrasonography.

In patients with discordant AC and MRI-derived PDFF, an element of hepatic hypofunction was associated with the discrepancy. This phenomenon may be a confounding factor for the high incidence of advanced fibrosis in patients with impaired liver function.

MRI-derived PDFF is more sensitive than the histologically determined steatosis grade for quantifying the grade of hepatic steatosis [31–33]. Theoretically, MRI-derived PDFF is unaffected by liver fibrosis [34]. However, the relationship between MRI-derived PDFF and histological status has been demonstrated to be differentially influenced by fibrosis stage, which contributes to difficulties in making a direct comparison between these two diagnostic methods [35]. Since most of what is known about the clinical phenotype and natural history of NAFLD is based on histology, it is important to interpret MRI-derived PDFF based on what is already known about the liver histology of NAFLD. Predicting histological hepatic steatosis grade from MRI-derived PDFF is one approach. In situations where there is a larger area of fibrosis in the pathological specimen, there will be fewer hepatocytes per slide.

However, the pathologist's report is still based on the percentage of hepatocytes that contain fat droplets. By contrast, MRI-derived PDFF measures the actual percentage of fat in the liver; thus, a reduction in the number of hepatocytes due to fibrosis will result in a large discrepancy between histological findings and MRI-derived PDFF [33,36]. Permutt et al. [36] demonstrated that the relationship between MRI-derived PDFF and steatosis grade based on histology remains relatively stable at fibrosis stages 0–3 but at stage 4. Idilman et al. [37] showed that the correlation between biopsy and steatosis as determined by MRI-derived PDFF was less pronounced when fibrosis was present (r=0.60) than when fibrosis was absent (r=0.86, P=0.02) [37]. In our study, ACs were high in patients with no hepatic steatosis (MRI-derived PDFF <5.2%) and high liver stiffness (MR elastography value ≥6.7 kPa); this phenomenon was considered to be due to US attenuation caused by liver fibrosis. The aim of this study is to raise alarm about this phenomenon. In addition, we have considered it useful to conduct two-dimensional share wave elastography (2D-SWE) simultaneously with AC measurement. We have previously demonstrated a strong correlation between MR elastography and 2D-SWE values in approximately 1,000 patients [38]. Therefore, it is important to measure 2D-SWE values at the same time as AC measurement and use the 2D-SWE value as a reference to determine the degree of hepatic steatosis.

This study has some limitations. First, histological support with liver biopsy was not available for this study. We only used MR elastography value as an indicator of liver fibrosis. In the presence of inflammation and ballooning, elastic modulus is high due to increased intra-tissue pressure caused by increased regional blood flow, congestive edema, and inflammatory cell infiltration; the interpretation of liver stiffness measurement changes must account for these effects [39]. Future studies with histological evaluation of fibrosis are necessary. Second, the majority of study participants had chronic liver disease or advanced age. Future studies including patients with acute liver disease and young age are necessary.

In conclusion, we demonstrated that AC is affected by the grade of hepatic fibrosis in patients without hepatic steatosis. ACs should be interpreted with caution in patients with advanced liver fibrosis who do not have steatosis. Future studies are needed to assess this relationship in various types of liver diseases and age groups.

ORCID: Takashi Kumada: https://orcid.org/0000-0003-2211-495X; Hidenori Toyoda: https://orcid.org/0000-0002-1652-6168; Sadanobu Ogawa: https://orcid.org/0000-0002-2916-5875; Tatsuya Gotoh: https://orcid.org/0000-0002-8097-0757; Yasuaki Suzuki: https://orcid.org/0000-0001-7081-5625; Kento Imajo: https://orcid.org/0000-0002-1931-6326; Katsutoshi Sugimoto: https://orcid.org/0000-0001-6271-7806; Tatsuya Kakegawa: https://orcid.org/0000-0001-7776-4795; Hidekatsu Kuroda: https://orcid.org/0000-0002-1471-1087; Yutaka Yasui: https://orcid.org/0000-0002-6117-4990; Nobuharu Tamaki: https://orcid.org/0000-0003-4634-6616; Masayuki Kurosaki: https://orcid.org/0000-0001-7016-8931; Namiki Izumi: https://orcid.org/0000-0002-0055-8229; Tomoyuki Akita: https://orcid.org/0000-0002-1056-3611; Junko Tanaka: https://orcid.org/0000-0002-5669-4051; Atsushi Nakajima: https://orcid.org/0000-0002-6263-1436

※ Author affiliations

[1]Department of Nursing, Faculty of Nursing, Gifu Kyoritsu University, Ogaki; [2]Department of Gastroenterology and Hepatology, Ogaki Municipal Hospital, Ogaki; [3]Department of Imaging Diagnosis, Ogaki Municipal Hospital, Ogaki; [4]Department of Gastroenterology, Nayoro City General Hospital, Nayoro; [5]Department of Gastroenterology, Yokohama City University Graduate School of Medicine, Yokohama; [6]Department of Gastroenterology, Shin-yurigaoka General Hospital, Kawasaki; [7]Department of Gastroenterology and Hepatology, Tokyo Medical University, Tokyo; [8]Division of Hepatology, Department of Internal Medicine, Iwate Medical University, Morioka; [9]Department of Gastroenterology and Hepatology, Musashino Red Cross Hospital, Musashino-shi; [10]Department of Epidemiology, Infectious Disease Control, and Prevention, Hiroshima University Institute of Biomedical and Health Sciences, Hiroshima, Japan

Author Contributions

Conceptualization: Kumada T. Data acquisition: Toyoda H, Ogawa S, Gotoh T, Suzuki Y, Imajo K, Sugimoto K, Kakegawa T, Kuroda H, Yasui Y, Tamaki N, Kurosaki M. Data analysis or interpretation: Ogawa S, Gotoh T, Toyoda H. Drafting of the manuscript: Kumada T. Critical revision of the manuscript: Kumada T, Toyoda H, Ogawa S, Gotoh T, Suzuki Y, Imajo K, Sugimoto K, Kakegawa T, Kuroda H, Yasui Y, Tamaki N, Kurosaki M, Izumi N, Akita T, Tanaka J, Nakajima A. Approval of the final version of the manuscript: all authors.

Conflict of Interest

Takashi Kumada has received research grants from GE Healthcare. Hidenori Toyoda, Sadanobu Ogawa, Tatsuya Goto, Yasuaki Suzuki, Kento Imajo, Katsutoshi Sugimoto, Tatsuya Kakegawa, Hidekatsu Kuroda, Yutaka Yasui, Nobuharu Tamaki, Masayuki Kurosaki, Namiki Izumi, Tomoyuki Akita, Junko Tanaka, and Atsushi Nakajima declare that they have no conflicts of interest.

Acknowledgments

This work has been supported by grant funding and a loan of equipment from GE Healthcare. The authors thank Naohisa Kamiyama, PhD; Takuma Oguri, PhD; and Nauchi Akihito, who are employees of GE Healthcare, for their technical support.

Supplementary Material

Supplementary Table 1. Intrarater and interrater reliability of the US

attenuation parameter (https://doi.org/10.14366/usg.23194).

Supplementary Table 2. Multiple comparison using the Steel-Dwass test among groups A, B, and C, which showed significant differences by the Kruskal-Wallis test in Table 2 (https://doi.org/10.14366/usg.23194).

References

1. Eguchi Y, Hyogo H, Ono M, Mizuta T, Ono N, Fujimoto K, et al. Prevalence and associated metabolic factors of nonalcoholic fatty liver disease in the general population from 2009 to 2010 in Japan: a multicenter large retrospective study. J Gastroenterol 2012;47:586-595.
2. Makuza JD, Jeong D, Binka M, Adu PA, Cua G, Yu A, et al. Impact of hepatitis B virus infection, non-alcoholic fatty liver disease, and hepatitis C virus co-infection on liver-related death among people tested for hepatitis B virus in British Columbia: results from a large longitudinal population-based cohort study. Viruses 2022;14:2579.
3. El-Badry AM, Breitenstein S, Jochum W, Washington K, Paradis V, Rubbia-Brandt L, et al. Assessment of hepatic steatosis by expert pathologists: the end of a gold standard. Ann Surg 2009;250:691-697.
4. Bonekamp S, Tang A, Mashhood A, Wolfson T, Changchien C, Middleton MS, et al. Spatial distribution of MRI-Determined hepatic proton density fat fraction in adults with nonalcoholic fatty liver disease. J Magn Reson Imaging 2014;39:1525-1532.
5. Ratziu V, Charlotte F, Heurtier A, Gombert S, Giral P, Bruckert E, et al. Sampling variability of liver biopsy in nonalcoholic fatty liver disease. Gastroenterology 2005;128:1898-1906.
6. Loomba R, Sirlin CB, Ang B, Bettencourt R, Jain R, Salotti J, et al. Ezetimibe for the treatment of nonalcoholic steatohepatitis: assessment by novel magnetic resonance imaging and magnetic resonance elastography in a randomized trial (MOZART trial). Hepatology 2015;61:1239-1250.
7. Neuschwander-Tetri BA, Loomba R, Sanyal AJ, Lavine JE, Van Natta ML, Abdelmalek MF, et al. Farnesoid X nuclear receptor ligand obeticholic acid for non-cirrhotic, non-alcoholic steatohepatitis (FLINT): a multicentre, randomised, placebo-controlled trial. Lancet 2015;385:956-965.
8. European Association for the Study of the Liver; European Association for the Study of Diabetes; European Association for the Study of Obesity. EASL-EASD-EASO clinical practice guidelines for the management of non-alcoholic fatty liver disease. Obes Facts 2016;9:65-90.
9. Imajo K, Toyoda H, Yasuda S, Suzuki Y, Sugimoto K, Kuroda H, et al. Utility of ultrasound-guided attenuation parameter for grading steatosis with reference to MRI-PDFF in a large cohort. Clin Gastroenterol Hepatol 2022;20:2533-2541.
10. Dioguardi Burgio M, Ronot M, Reizine E, Rautou PE, Castera L, Paradis V, et al. Quantification of hepatic steatosis with ultrasound: promising role of attenuation imaging coefficient in a biopsy-proven cohort. Eur Radiol 2020;30:2293-2301.
11. Sasso M, Tengher-Barna I, Ziol M, Miette V, Fournier C, Sandrin L, et al. Novel controlled attenuation parameter for noninvasive assessment of steatosis using Fibroscan((R)): validation in chronic hepatitis C. J Viral Hepat 2012;19:244-253.
12. Jang JK, Kim SY, Yoo IW, Cho YB, Kang HJ, Lee DH. Diagnostic performance of ultrasound attenuation imaging for assessing low-grade hepatic steatosis. Eur Radiol 2022;32:2070-2077.
13. Tada T, Kumada T, Toyoda H, Yasuda S, Sone Y, Hashinokuchi S, et al. Liver stiffness does not affect ultrasound-guided attenuation coefficient measurement in the evaluation of hepatic steatosis. Hepatol Res 2020;50:190-198.
14. Jang JK, Choi SH, Lee JS, Kim SY, Lee SS, Kim KW. Accuracy of the ultrasound attenuation coefficient for the evaluation of hepatic steatosis: a systematic review and meta-analysis of prospective studies. Ultrasonography 2022;41:83-92.
15. Kim PH, Cho YA, Yoon HM, Bak B, Lee JS, Jung AY, et al. Accuracy of attenuation imaging in the assessment of pediatric hepatic steatosis: correlation with the controlled attenuation parameter. Ultrasonography 2022;41:761-769.
16. Johnson PJ, Berhane S, Kagebayashi C, Satomura S, Teng M, Reeves HL, et al. Assessment of liver function in patients with hepatocellular carcinoma: a new evidence-based approach-the ALBI grade. J Clin Oncol 2015;33:550-558.
17. Sterling RK, Lissen E, Clumeck N, Sola R, Correa MC, Montaner J, et al. Development of a simple noninvasive index to predict significant fibrosis in patients with HIV/HCV coinfection. Hepatology 2006;43:1317-1325.
18. Zhao Y, Jia M, Zhang C, Feng X, Chen J, Li Q, et al. Reproducibility of ultrasound-guided attenuation parameter (UGAP) to the noninvasive evaluation of hepatic steatosis. Sci Rep 2022;12:2876.
19. Jeon SK, Lee JM, Joo I, Yoon JH. Assessment of the inter-platform reproducibility of ultrasound attenuation examination in nonalcoholic fatty liver disease. Ultrasonography 2022;41:355-364.
20. Ferraioli G, Raimondi A, De Silvestri A, Filice C, Barr RG. Toward acquisition protocol standardization for estimating liver fat content using ultrasound attenuation coefficient imaging. Ultrasonography 2023;42:446-456.
21. Seo DM, Lee SM, Park JW, Kim MJ, Ha HI, Park SY, et al. How many times should we repeat measurements of the ultrasound-guided attenuation parameter for evaluating hepatic steatosis? Ultrasonography 2023;42:227-237.
22. Kuroda H, Abe T, Fujiwara Y, Nagasawa T, Takikawa Y. Diagnostic accuracy of ultrasound-guided attenuation parameter as a noninvasive test for steatosis in non-alcoholic fatty liver disease. J Med Ultrason (2001) 2021;48:471-480.

23. Imajo K, Kessoku T, Honda Y, Tomeno W, Ogawa Y, Mawatari H, et al. Magnetic resonance imaging more accurately classifies steatosis and fibrosis in patients with nonalcoholic fatty liver disease than transient elastography. Gastroenterology 2016;150:626-637.
24. Kumada T, Toyoda H, Yasuda S, Sone Y, Ogawa S, Takeshima K, et al. Prediction of hepatocellular carcinoma by liver stiffness measurements using magnetic resonance elastography after eradicating hepatitis C virus. Clin Transl Gastroenterol 2021;12:e00337.
25. Glantz SA, Slinker BK. Multicollinearity and what to do about it. In: Glantz SA, Slinker BK, eds. Primer of applied regression and analysis of variance. New York: McGraw-Hill, 1990;181-238.
26. Kanda Y. Investigation of the freely available easy-to-use software 'EZR' for medical statistics. Bone Marrow Transplant 2013;48:452-458.
27. Parker KJ, Asztely MS, Lerner RM, Schenk EA, Waag RC. In-vivo measurements of ultrasound attenuation in normal or diseased liver. Ultrasound Med Biol 1988;14:127-136.
28. Lin T, Ophir J, Potter G. Correlation of ultrasonic attenuation with pathologic fat and fibrosis in liver disease. Ultrasound Med Biol 1988;14:729-734.
29. Suzuki K, Hayashi N, Sasaki Y, Kono M, Kasahara A, Fusamoto H, et al. Dependence of ultrasonic attenuation of liver on pathologic fat and fibrosis: examination with experimental fatty liver and liver fibrosis models. Ultrasound Med Biol 1992;18:657-666.
30. Poul SS, Parker KJ. Fat and fibrosis as confounding cofactors in viscoelastic measurements of the liver. Phys Med Biol 2021;66:045024.
31. Raptis DA, Fischer MA, Graf R, Nanz D, Weber A, Moritz W, et al. MRI: the new reference standard in quantifying hepatic steatosis? Gut 2012;61:117-127.
32. Noureddin M, Lam J, Peterson MR, Middleton M, Hamilton G, Le TA, et al. Utility of magnetic resonance imaging versus histology for quantifying changes in liver fat in nonalcoholic fatty liver disease trials. Hepatology 2013;58:1930-1940.
33. Bannas P, Kramer H, Hernando D, Agni R, Cunningham AM, Mandal R, et al. Quantitative magnetic resonance imaging of hepatic steatosis: validation in ex vivo human livers. Hepatology 2015;62:1444-1455.
34. Yokoo T, Serai SD, Pirasteh A, Bashir MR, Hamilton G, Hernando D, et al. Linearity, bias, and precision of hepatic proton density fat fraction measurements by using MR imaging: a meta-analysis. Radiology 2018;286:486-498.
35. Schwimmer JB, Middleton MS, Behling C, Newton KP, Awai HI, Paiz MN, et al. Magnetic resonance imaging and liver histology as biomarkers of hepatic steatosis in children with nonalcoholic fatty liver disease. Hepatology 2015;61:1887-1895.
36. Permutt Z, Le TA, Peterson MR, Seki E, Brenner DA, Sirlin C, et al. Correlation between liver histology and novel magnetic resonance imaging in adult patients with non-alcoholic fatty liver disease - MRI accurately quantifies hepatic steatosis in NAFLD. Aliment Pharmacol Ther 2012;36:22-29.
37. Idilman IS, Aniktar H, Idilman R, Kabacam G, Savas B, Elhan A, et al. Hepatic steatosis: quantification by proton density fat fraction with MR imaging versus liver biopsy. Radiology 2013;267:767-775.
38. Kakegawa T, Sugimoto K, Kuroda H, Suzuki Y, Imajo K, Toyoda H, et al. Diagnostic accuracy of two-dimensional shear wave elastography for liver fibrosis: a multicenter prospective study. Clin Gastroenterol Hepatol 2022;20:e1478-e1482.
39. Tsujita Y, Sofue K, Ueshima E, Ueno Y, Hori M, Murakami T. Clinical application of quantitative MR imaging in nonalcoholic fatty liver disease. Magn Reson Med Sci 2023;22:435-445.